J Neurooncol (2010) 96:385–392
DOI 10.1007/s11060-009-9970-9

CLINICAL STUDY - PATIENT STUDY

Cellularity and apparent diffusion coefficient in oligodendroglial tumours characterized by genotype

Michael D. Jenkinson · Daniel G. du Plessis · Trevor S. Smith · Andrew R. Brodbelt · Kathy A. Joyce · Carol Walker

Received: 6 May 2009 / Accepted: 6 July 2009 / Published online: 19 July 2009

Abstract *Purpose* Apparent diffusion coefficient (ADC) describes water diffusion within tissues. Previous studies report a negative linear correlation between minimum ADC and tumour cellularity in different types of gliomas, but there are no studies in oligodendroglial tumours. This study evaluated the relationship between ADC and tumour cellularity in oligodendroglial tumours characterized by genotype. *Methods* ADC was assessed in 17 patients with known 1p/19q status: 3 grade II oligodendrogliomas (OII), 9 grade II oligoastrocytomas (OAII), 5 grade III oligoastrocytomas (OAIII). Regions of interest were placed on ADC maps around tumour margins to generate mean tumour ADC, and over minimum and maximum tumour ADC. Histopathology assessment of tumour cellularity determined minimum, maximum and mean cell density in serial stereotactic biopsies. *Results* 1p/19q loss was present in 2/3 OII, 5/9 OAII, 2/5 OAIII. Grade III tumours had higher maximum cell density than grade II tumours (17.2 vs. 10.57%: *Mann Whitney U*; ***P* = 0.20**). Oligoastrocytoma were more likely to have a lower minimum cell density than oligodendrogliomas (*Mann Whitney U*; ***P* = 0.032**). There was no relationship between cell density and genotype. There was no linear correlation between mean ADC and mean cell density (*Spearman's rho;* $r = 0.486$: $P = 0.438$), minimum ADC and maximum cell density (*Spearman's rho;* $r = 0.158$: $P = 0.660$), and maximum ADC and minimum cell density (*Spearman's rho;* $r = 0.039$: $P = 0.985$). *Conclusions* In oligodendroglial tumours there is no relationship between quantitative assessment of cellularity and ADC. This may reflect differences in oligodendroglial tumour biology compared to other gliomas, although the composition of the extracellular matrix may influence ADC more than cellularity.

Keywords Oligodendroglial tumour · ADC · Cellularity · Genotype

M. D. Jenkinson (✉) · A. R. Brodbelt
Department of Neurosurgery, The Walton Centre for Neurology and Neurosurgery, Lower Lane, Liverpool L9 7LJ, UK
e-mail: michael.jenkinson@liv.ac.uk

T. S. Smith
Department of Neuroradiology, The Walton Centre for Neurology and Neurosurgery, Liverpool L9 7LJ, UK

D. G. du Plessis
Department of Neuropathology, Hope Hospital, Manchester M6 8HD, UK

M. D. Jenkinson · K. A. Joyce · C. Walker
School of Cancer Studies, University of Liverpool, Liverpool L3 9TA, UK

Introduction

Diffusion-weighed imaging (DWI) affords the opportunity to assess free-water movement in tissues and relates image intensity to the relative mobility of water molecules. In the brain, true diffusion is beyond the spatial resolution of MRI, therefore using a statistical model the apparent diffusion coefficient (ADC), which describes microscopic water diffusion, can be recorded for each voxel and displayed on an ADC map. A low ADC results from high signal intensity on DWI and indicates restricted diffusion, whereas a high ADC results from low signal intensity and indicates free diffusion [1]. Since ADC is not a measure of true diffusion, its relationship with the underlying tissue architecture has been the subject of several studies. It has been reported that smaller ADC values correspond with the most cellular tumour component, whilst larger ADC values

are correlated with low cellularity [2, 3]. The minimum ADC values are therefore thought to represent the most cellular tumour component, indeed low-grade gliomas tend to have higher ADC values than high-grade gliomas [4].

ADC maps have many potential applications in neuro-oncology, including tumour classification [4–6], assessing response to therapy and identifying tumour recurrence [7–9]. However, there are few reports of ADC analysis of oligodendroglial tumours in the current literature [9, 10]. The biological factors responsible for differential chemosensitivity in oligodendroglial tumours with and without 1p/19q loss are not known. Previous studies have sought to characterize these clinical differences and distinguish the molecular subtypes of oligodendroglial tumours on both conventional [11, 12] and advanced MRI [13]. In a previous study we reported differences in ADC and ATC (ADC transition coefficient: the rate of change in ADC between adjacent voxels traversing the tumour border) between oligodendroglial tumour genotypes, but not between oligodendroglial histopathology subtypes and grade [14]. Tumours with intact 1p/19q had higher maximum and histogram ADC, and greater ATC compared to those with 1p/19q loss, but the relationship to the underlying tissue architecture was not investigated. Therefore the aim of this study was to investigate the relationship between tumour ADC and histopathology assessment of cellularity in oligodendroglial tumours characterised by genotype.

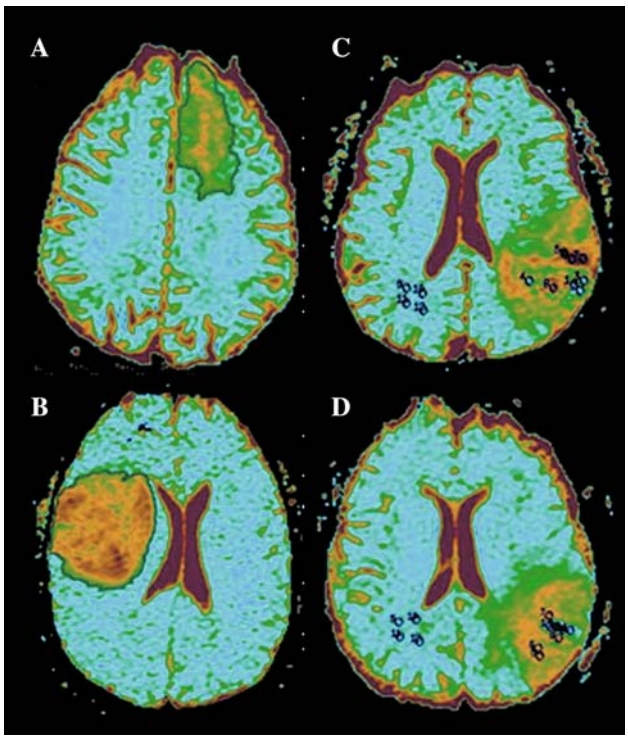

Fig. 1 **a–b** ADC maps showing a non-geometric region of interest around the tumour margin. **a** OAII with 1p/19q loss (ADC: $1.63 \pm 0.28 \times 10^{-3}$ mm^2/s (mean ± SD)) and **b** OAII with intact 1p/19q ($1.27 \pm 0.18 \times 10^{-3}$ mm^2/s). **c–d** ADC maps showing ROI placement over minimum (1–4), maximum (5–8) and normal (9–12) brain in **c.** (Adapted from Jenkinson et al. 2007 with permission [14])

Materials and methods

Case selection

Patients were drawn from a prospective study of adult oligodendroglial tumours between July 2001 and June 2004 [15–18]. Patients were included in this study if they met the following criteria: (i) histopathology diagnosis of oligodendroglioma (O) or oligoastrocytoma (OA) World Health Organisation (WHO) grade II or III [19]; (ii) known 1p/19q status; and (iii) had diffusion-weighted imaging (DWI) performed pre- (n = 6) or post-biopsy (n = 11), but prior to commencing current therapy; all were included in our previous study [14]. All patients underwent serial stereotactic biopsy for diagnostic purposes. The study had ethical approval.

MR imaging protocol and post-processing

Diffusion-weighted echoplanar imaging (TR = 9,400 ms, TE 97 ms, matrix size 160 × 128, FOV 300 × 190 mm, thickness = 5 mm, b = 0 and 1,000 s/mm^2) were obtained using a 1.5-T Signa MR Scanner (GE Medical Systems). Images were post-processed offline using commercial software (Functool2 [v 6.0], Sun Microsystems) to generate an ADC map. Evaluation of ADC was carried out as previously described [14]. Briefly, regions of interest (ROI) were independently placed by a neurosurgeon (MDJ) and a neuro-radiologist (TSS) blinded to histopathology subtype and genotype. ADC values within each tumour were assessed by placement of ROI according to previously published methods with low inter- and intra-observer variation [13]. The following protocol was used: first, using the axial slice with the greatest abnormal ADC area, a non-geometric ROI was drawn around the tumour margin (excluding cystic and necrotic areas) to generate the mean ADC value (±standard deviation). Second, four circular ROIs (area: 22 mm^2) were placed over regions representative of maximum and minimum tumour ADC and over contralateral normal brain (Fig. 1). The mean of each group of four ROI was used for comparison between tumour and normal brain and with cellularity and genotype.

Histopathology assessment

Serial stereotactic biopsy provides tissue samples at 1 mm intervals along a trajectory from the radiological tumour margin to a target point within the volumetric centre that

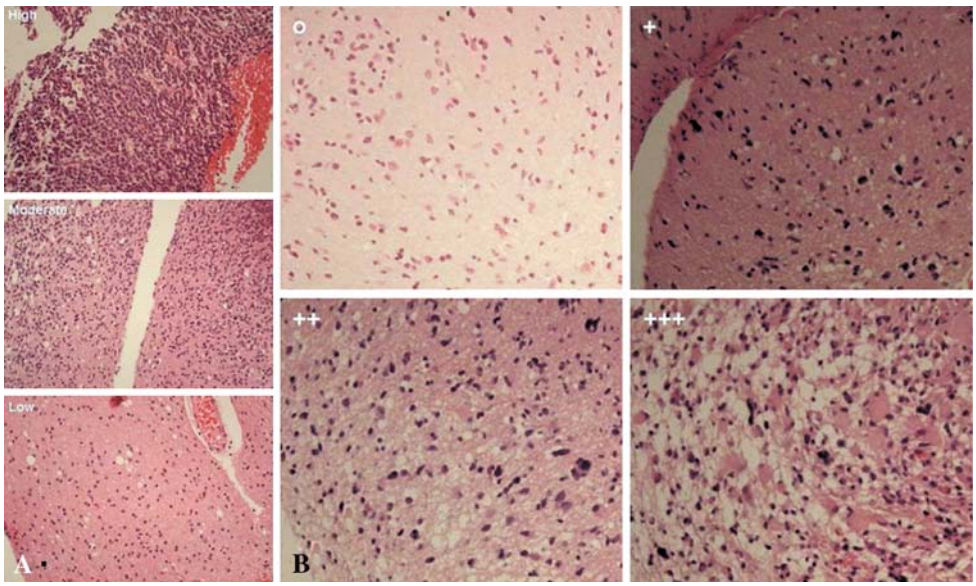

Fig. 2 **a** Cellularity was classified as: high—tumour cells adjacent to each other with little or no intervening parenchyma; moderate—some tumour cells may be adjacent to each other but less densely packed; low—few tumour cells with intervening parenchyma (×200 original magnification). **b** Photographs of a grade III oligoastrocytoma showing the typical features used to assign microcystic component (original magnification ×200). Microcysts were classified as: no microcysts (o); scant small cysts (+); more widespread small cysts (++); and large widespread cysts (+++)

encompasses areas of contrast enhancement. Routinely processed haematoxylin and eosin (H&E) stained paraffin embedded tissue samples from serial stereotactic biopsies were used to assess histopathology features by an experienced neuropathologist (DduP) [12]. The cellularity of each sample was assessed (Fig. 2a) as either high: tumour cells adjacent to each other with little or no intervening parenchyma; moderate: some tumour cells may be adjacent to each other but less densely packed; or low: few tumour cells with intervening parenchyma. The background matrix was assessed to determine the presence and extent of microcystic change. The following scoring system was applied to each sample to assess microcysts: (Fig. 2b): no microcysts (o); scant small cysts (+); more widespread small cysts (++); and large widespread cysts (+++). The computed cell density was calculated according to published methods [3]. Slides were reviewed at ×200 original optical magnification. A digital colour photograph was taken of the ×200 image and converted to a greyscale image using Paint Shop Pro 7 (Corel). Uncompressed greyscale tiff images for each biopsy sample were analyzed using the public domain National Institutes of Health (NIH) Image program v1.61 (http://rsb.info.nih.gov/nih-image/). Each image was converted to a black and white binary image by setting the image threshold at a value at which cell nuclei were coloured red but the surrounding tissue was not. The border of the tumour specimen was ringed in those biopsy samples that did not fill the entire image and the area outside the marked shape was excluded from the analysis. Histogram analysis of the binary image identified the number of cell nuclei pixels (black) and the background non-nuclei pixels (white). The cell density for each biopsy was defined as the number of nuclei pixels divided by the total number of pixels in within the biopsy margin, and expressed as a percentage (Fig. 3). For each case the average cell density was calculated by summing the cell density of each biopsy and dividing by the number of biopsies per case. The biopsy with the lowest and highest cell density for each case was recorded as the minimum and maximum cell density respectively (Table 1).

Data analysis and statistics

The raw data for each biopsy sample was analyzed to determine any associations between the computed cell density and visual histopathology features. To enable comparison of histopathology features with molecular genetics and ADC a summary of the data for each patient was created (Table 2). Microcystic change for each case was categorized as present: >50% of biopsy samples with microcysts and at least one sample with ++; or absent: <50% of biopsy samples with microcysts and no samples

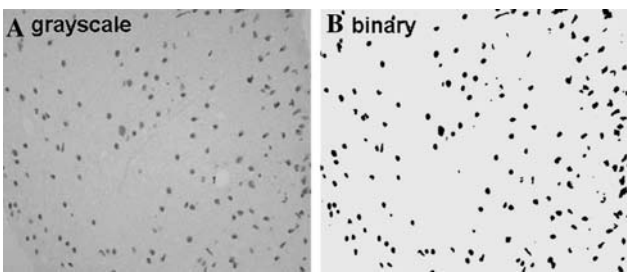

Fig. 3 Photographs of a grade II oligoastrocytoma showing **a** grayscale and **b** binary images (original magnification ×200) from which the number of black and white pixels were calculated. The percentage cell density is the number of black pixels (54,583) divided by the total pixel count (1,339,000) multiplied by 100 (4.08%)

Table 1 Summary histopathology assessment and ADC data for each case

Case	Number of biopsies	Microcyst	Number of samples with cellularity:			Cell density			ADC (mean [SD])				Subtype and genotype	
			Low	Moderate	High	Average	Maximum	Minimum	Minimum	Maximum	Normal	Histogram mean	Subtype and grade	1p/19q loss
o-01	7	No	3	2	2	7.04	13.82	2.01	0.59 [0.05]	1.72 [0.06]	0.84 [0.07]	1.19 [0.31]	OAIII	No
o-02	8	No	2	6	0	7.73	10.91	5.20	0.47 [0.08]	1.75 [0.09]	0.82 [0.07]	1.27 [0.27]	OII	No
o-03	6	No	4	2	0	6.81	8.73	4.50	1.06 [0.07]	1.61 [0.05]	0.79 [0.05]	1.42 [0.17]	OAII	No
o-04	6	Yes	1	5	0	8.25	17.20	3.78	1.16 [0.14]	1.97 [0.02]	0.80 [0.03]	1.54 [0.25]	OAIII	No
o-05	6	No	0	3	3	17.35	20.68	13.20	1.35 [0.07]	2.36 [0.13]	0.78 [0.07]	1.54 [0.33]	OAIII	No
o-06	5	No	5	0	0	4.39	5.51	3.56	1.34 [0.08]	1.96 [0.04]	0.71 [0.05]	1.63 [0.28]	OAII	No
o-07	6	Yes	1	3	2	9.25	14.72	3.05	1.19 [0.05]	2.08 [0.10]	0.76 [0.06]	1.71 [0.30]	OAII	No
o-08	7	Yes	1	6	0	8.51	10.22	6.24	1.22 [0.07]	1.66 [0.02]	0.72 [0.04]	1.82 [0.39]	OAII	No
o-09	7	Yes	1	6	0	7.37	11.62	4.75	0.82 [0.04]	1.38 [0.09]	0.67 [0.08]	1.11 [0.26]	OAII	Yes
o-10	7	Yes	4	3	0	5.51	8.47	1.85	0.95 [0.14]	1.28 [0.03]	0.69 [0.08]	1.12 [0.14]	OAII	Yes
o-11	8	Yes	4	4	0	5.88	11.66	2.07	0.88 [0.10]	1.50 [0.06]	0.59 [0.07]	1.16 [0.21]	OAII	Yes
o-12	8	Yes	2	6	0	6.80	9.79	4.78	0.79 [0.04]	1.66 [0.09]	0.78 [0.03]	1.27 [0.18]	OAII	Yes
o-13	3	Yes	0	0	3	21.42	23.88	16.73	1.11 [0.09]	1.44 [0.06]	0.73 [0.07]	1.27 [0.28]	OII	Yes
o-14	6	Yes	2	2	2	11.33	16.73	5.32	1.06 [0.07]	1.48 [0.05]	0.64 [0.06]	1.29 [0.20]	OAIII	Yes
o-15	5	No	1	3	1	13.61	26.35	3.44	0.77 [0.05]	1.92 [0.15]	0.67 [0.05]	1.31 [0.24]	OAIII	Yes
o-16	4	Yes	0	1	3	15.40	18.25	11.55	0.90 [0.17]	1.82 [0.16]	0.80 [0.03]	1.32 [0.25]	OII	Yes
o-17	4	No	3	1	0	5.10	6.51	4.04	1.20 [0.08]	1.74 [0.06]	0.82 [0.05]	1.35 [0.22]	OAII	Yes

Table 2 Correlations between subtype, grade and genotype and **A.** microcysts; **B.** average, maximum and minimum cell density (**Fisher's Exact test*; $^{+}$*Mann Whitney U test*)

A.		Microcysts		*P**
		No	Yes	
Subtype	O	1	2	1.0
	OA	6	8	
Grade	II	4	8	0.593
	III	3	2	
1p/19q loss	No	5	3	0.153
	Yes	2	7	

B.		Average cell density median (range)	P^{+}	Maximum cell density median (range)	P^{+}	Minimum cell density median (range)	P^{+}
Subtype	O	15.4 (7.73–21.42)	0.078	18.25 (10.91–23.88)	0.206	11.55 (5.20–16.37)	0.032
	OA	7.21 (4.39–21.42)		11.64 (5.51–26.35)		3.91 (1.85–13.20)	
Grade	II	7.10 (4.39–21.42)	0.114	10.57 (5.51–23.88)	0.020	4.63 (1.85–16.73)	0.883
	III	11.33 (7.04–17.35)		17.20 (13.82–26.35)		3.78 (2.01–13.20)	
1p/19q loss	No	8.00 (4.39–17.35)	1.0	12.37 (5.51–20.68)	0.630	4.14 (2.01–13.20)	0.847
	Yes	7.37 (5.10–21.42)		11.66 (6.51–26.35)		4.75 (1.85–16.73)	

with ++. The average of the computed cell density for each case was calculated and the minimum and maximum cell density was also recorded. The summary data were compared to histopathology and molecular genetics, and minimum, maximum and mean histogram ADC. Due to the small sample size non-parametric statistical tests were used (Mann Whitney U, Fisher's Exact and Spearman's rho tests). Data was analyzed using SPSS software.

Results

Study population

As previously described [14], 17 cases were studied (11 male; 6 female). Median age at operation was 42 years (range: 24–72 years). There were fourteen primary, previously untreated cases. Three recurrent tumours had received radiotherapy prior to MRI (median 64 months; range: 51–71). 1p/19q loss was present in 2/3 OII, 5/9 OAII and 2/5 OAIII.

Histopathology parameters

The median number of biopsy samples assessed per case was six (range 3–8). Varying levels of heterogeneity of cellularity, microcysts and cell density were seen for each case. Using the data from each biopsy sample the computed cell density was compared to the visual pathology assessments of cellularity and the presence or absence of microcysts. Computed cell density showed good separation when categorized as low, moderate or high cellularity (Fig. 4a). Cell density did not significantly differ between samples with or without microcysts (Fig. 4b). Oligodendrogliomas and oligoastrocytomas of both grades and genotypes were equally likely to have microcysts (Table 2). Oligoastrocytomas were more likely to have a lower minimum cell density than oligodendrogliomas (*Mann Whitney U;* ***P* = 0.032**). Grade III tumours had a higher maximum cell density than grade II tumours (*Mann Whitney U;* ***P* = 0.020**). Tumours with or without 1p/19q loss had similar average, minimum and maximum cell density (Table 2).

Histopathology, cell density and ADC

Tumours with or without microcysts were equally likely to show high or low mean histogram, maximum and minimum ADC values (Fig. 5). There was no linear correlation between mean histogram ADC and average cell density (Fig. 6a), minimum ADC and maximum cell density (Fig. 6b), and maximum ADC and minimum cell density (Fig. 6c).

Discussion

This is the first study to investigate the relationship between ADC and cellularity in a series of oligodendroglial tumours characterised by genotype. Oligodendroglial tumours with 1p/19q loss were more likely to have a lower maximum ADC, and a lower mean histogram ADC compared to those with intact 1p/19q, however ADC was not

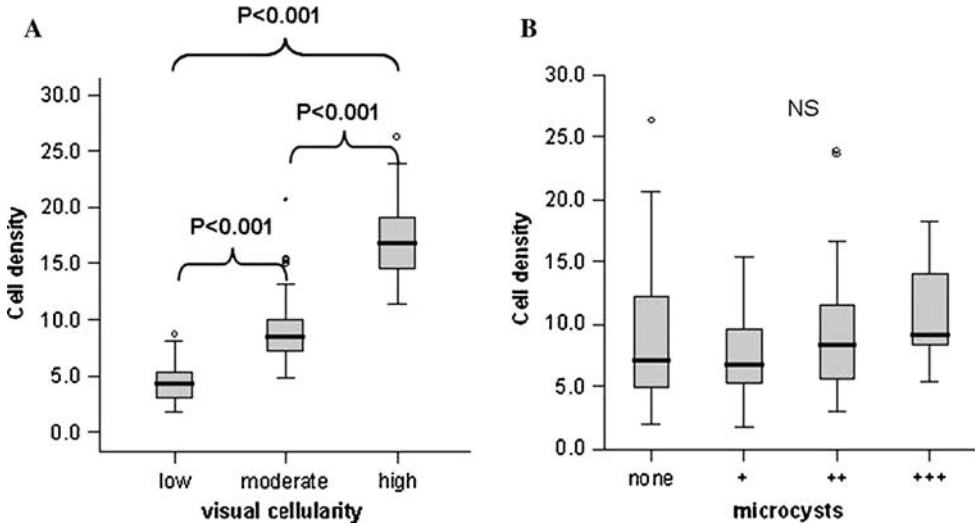

Fig. 4 Boxplots of computed cell density and parameters assessed visually: **a** cellularity, **b** microcysts (*Mann Whitney U test*). *NS* non-significant

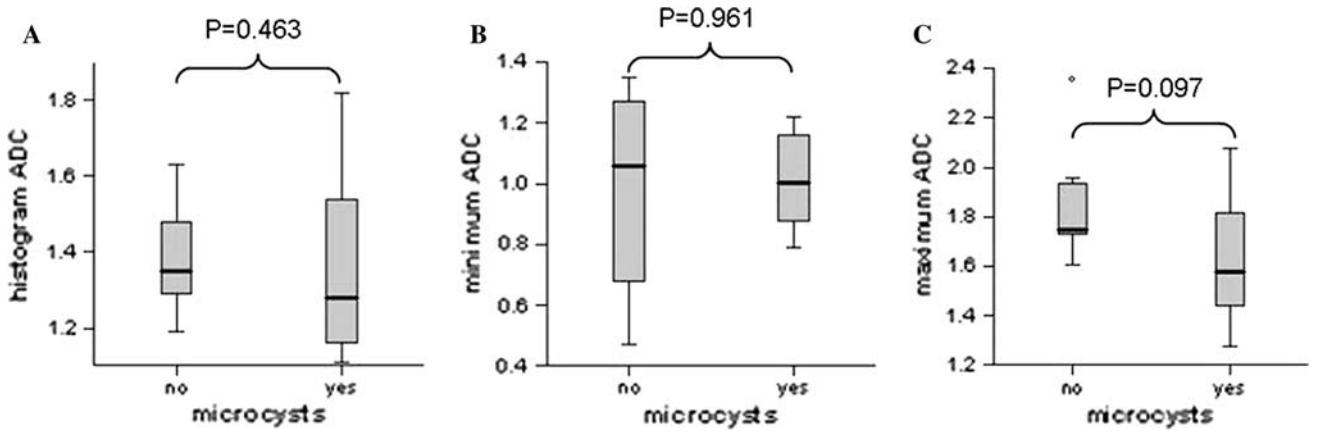

Fig. 5 Boxplots of histogram, minimum and maximum ADC and **a–c** presence or absence of microcysts (*Mann Whitney U test*)

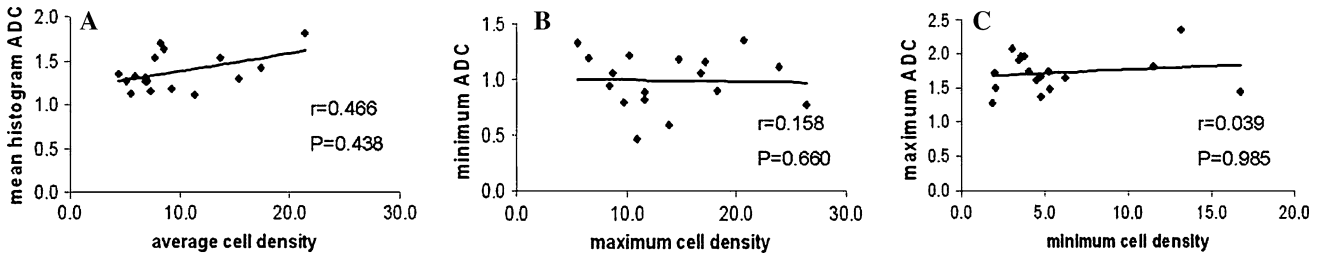

Fig. 6 Scatterplots showing no linear correlation between **a** mean histogram ADC and average cell density; **b** minimum ADC and maximum cell density and; **c** maximum ADC and minimum cell density (*Spearman's rho correlation*)

significantly different between histopathology subtypes or grades. Categorization of cases as low, moderate and high cellularity showed good agreement with computed cell density, and regardless of subtype, grade or genotype, tumours were equally likely to have low, moderate and high cellularity. Grade III tumours had a higher maximum cell density than grade II tumours. Oligoastrocytomas had a lower minimum cell density than oligodendrogliomas. There was no linear correlation between histogram ADC and mean cell density, minimum ADC and maximum cell density, and maximum ADC and minimum cell density. The presence or absence of microcysts was unrelated to tumour ADC.

The apparent diffusion coefficient, which separates diffusion-weighted signal change from T2-weighted signal change [20], is used as a surrogate measure of water

movement within the brain. The relationship between ADC and the corresponding tissue architecture is unknown but two studies have suggested that it may be related to cell density [2, 3]. Both studies investigated the relationship between ADC and cell density in small mixed cohorts of gliomas (including glioblastomas, anaplastic astrocytomas, diffuse astrocytomas and oligodendrogliomas) and surgical specimens that were retrospectively correlated with ADC values. Minimum ADC values showed a negative linear correlation with tumour cellularity, such that free water diffusion decreased with increasing cell density, however, this relationship was not observed in our study. There was also no linear correlation between maximum tumour ADC and minimum cell density or the degree of microcystic change, which might be expected as water diffusion has been suggested to be greater in areas with necrosis and microcysts [3]. As in previous studies [2, 3], the correlation between cell density and ADC was a retrospective analysis, samples were not co-registered with surgical planning MRI and all three series had small patient numbers ($n = 17–20$). There was no correlation between ADC and cellularity in this study, which may reflect the fact that previous studies also included high-grade gliomas [2, 3]. However, if cellularity is the primary determinant of ADC, then tumours, which show increased cellularity, should have a lower ADC than normal brain. This was not the case in our study, and suggests that factors other than cellularity influence ADC; indeed it has been shown that the composition of the extracellular matrix may influence water diffusion. Compared to normal white matter, both astrocytomas and oligodendroglial tumours contain increased amounts the glycosaminoglycan hyaluronan [21, 22], which exhibits a positive correlation with ADC [22].

ADC values represent diffusion along a single gradient however diffusion is a three-dimensional process. Diffusion tensor imaging (DTI) measures water movement in multiple directions to provide data on both rate and direction. Since water movement is anisotropic, one of the units of measure is fractional anisotropy (FA). In a series of patients with glioblastoma there was good correlation between tumour FA and cell density, though the data was derived from retrospective image correlation [23]. Two studies investigating the relationship between tumour tissue architecture and fractional anisotropy using three-dimensional stereotactic planning MRI co-registered and prospectively fused with DTI have recently been published [24, 25]. In the first, tumour cell number showed a logarithmic relationship with FA values, such that there was greater diffusion in areas of low cell number compared to those with higher cell numbers. The study authors hypothesized that this reflected the infiltration invasion mechanism of gliomas, namely, preserved fiber tracts at the tumour border with enlargement of the extracellular space [25]. In the second image-guided biopsy study, a correlative analysis was performed between tissue architecture (classified as solid tumour, tumour infiltrating normal brain, or normal brain) determined from biopsy specimens and diffusion tensor imaging characteristics [24]. Solid tumour had a different diffusion tensor tissue signature compared to infiltrated normal brain, and to normal brain. The diffusion tensor tissue signatures extended beyond the T2 tumour margin in half the cases examined [24]. A similar study has yet to be performed using ADC, and its relationship to tissue architecture remains speculative.

Conclusions

The absence of a positive linear correlation between ADC and cellularity reported herein highlights the need for further study using image guided sampling and intra-operative image registration to related tissue biology to ADC in oligodendroglial tumours and improve the diagnostic utility of ADC maps.

Acknowledgments Supported by grants from The Walton Centre Neuroscience Fund, Clatterbridge Cancer Research Trust and The Royal Colleges of Edinburgh and Ireland.

Conflict of interest statement We declare that we have no conflict of interest.

References

1. Le Bihan D, Poupon C, Amadon A, Lethimonnier F (2006) Artifacts and pitfalls in diffusion MRI. J Magn Reson Imaging 24:478–488
2. Gupta RK, Cloughesy TF, Sinha U, Garakian J, Lazareff J, Rubino G, Rubino L, Becker DP, Vinters HV, Alger JR (2000) Relationships between choline magnetic resonance spectroscopy, apparent diffusion coefficient and quantitative histopathology in human glioma. J Neurooncol 50:215–226
3. Sugahara T, Korogi Y, Kochi M, Ikushima I, Shigematu Y, Hirai T, Okuda T, Liang L, Ge Y, Komohara Y, Ushio Y, Takahashi M (1999) Usefulness of diffusion-weighted MRI with echo-planar technique in the evaluation of cellularity in gliomas. J Magn Reson Imaging 9:53–60
4. Kono K, Inoue Y, Nakayama K, Shakudo M, Morino M, Ohata K, Wakasa K, Yamada R (2001) The role of diffusion-weighted imaging in patients with brain tumors. AJNR Am J Neuroradiol 22:1081–1088
5. Chiang IC, Kuo YT, Lu CY, Yeung KW, Lin WC, Sheu FO, Liu GC (2004) Distinction between high-grade gliomas and solitary metastases using peritumoral 3-T magnetic resonance spectroscopy, diffusion, and perfusion imagings. Neuroradiology 46:619–627
6. Yang D, Korogi Y, Sugahara T, Kitajima M, Shigematsu Y, Liang L, Ushio Y, Takahashi M (2002) Cerebral gliomas: prospective comparison of multivoxel 2D chemical-shift imaging proton MR spectroscopy, echoplanar perfusion and diffusion-weighted MRI. Neuroradiology 44:656–666

7. Chenevert TL, Stegman LD, Taylor JM, Robertson PL, Greenberg HS, Rehemtulla A, Ross BD (2000) Diffusion magnetic resonance imaging: an early surrogate marker of therapeutic efficacy in brain tumors. J Natl Cancer Inst 92:2029–2036
8. Hein PA, Eskey CJ, Dunn JF, Hug EB (2004) Diffusion-weighted imaging in the follow-up of treated high-grade gliomas: tumor recurrence versus radiation injury. AJNR Am J Neuroradiol 25:201–209
9. Jager HR, Waldman AD, Benton C, Fox N, Rees J (2005) Differential chemosensitivity of tumor components in a malignant oligodendroglioma: assessment with diffusion-weighted, perfusion-weighted, and serial volumetric MR imaging. AJNR Am J Neuroradiol 26:274–278
10. Tozer DJ, Jager HR, Danchaivijitr N, Benton CE, Tofts PS, Rees JH, Waldman AD (2007) Apparent diffusion coefficient histograms may predict low-grade glioma subtype. NMR Biomed 20:49–57
11. Megyesi JF, Kachur E, Lee DH, Zlatescu MC, Betensky RA, Forsyth PA, Okada Y, Sasaki H, Mizoguchi M, Louis DN, Cairncross JG (2004) Imaging correlates of molecular signatures in oligodendrogliomas. Clin Cancer Res 10:4303–4306
12. Jenkinson MD, du Plessis DG, Smith TS, Joyce KA, Warnke PC, Walker C (2006) Histological growth patterns and genotype in oligodendroglial tumours: correlation with MRI features. Brain 129:1884–1891
13. Jenkinson MD, Smith TS, Joyce KA, Fildes D, Broome J, du Plessis DG, Haylock B, Husband DJ, Warnke PC, Walker C (2006) Cerebral blood volume, genotype and chemosensitivity in oligodendroglial tumours. Neuroradiology 48:703–713
14. Jenkinson MD, Smith TS, Brodbelt AR, Joyce KA, Warnke PC, Walker C (2007) Apparent diffusion coefficients in oligodendroglial tumours characterised by genotype. J Magn Reson Imaging 26:1405–1412
15. Walker C, du Plessis DG, Fildes D, Haylock B, Husband D, Jenkinson MD, Joyce KA, Broome J, Kopitski K, Prosser J, Smith T, Vinjamuri S, Warnke PC (2004) Correlation of molecular genetics with molecular and morphological imaging in gliomas with an oligodendroglial component. Clin Cancer Res 10:7182–7191
16. Walker C, du Plessis DG, Joyce KA, Fildes D, Gee A, Haylock B, Husband D, Smith T, Broome J, Warnke PC (2005) Molecular pathology and clinical characteristics of oligodendroglial neoplasms. Ann Neurol 57:855–865
17. Walker C, Haylock B, Husband D, Joyce KA, Fildes D, Jenkinson MD, Smith T, Broome J, du Plessis DG, Warnke PC (2006) Clinical use of genotype to predict chemosensitivity in oligodendroglial tumors. Neurology 66:1661–1667
18. Walker C, Haylock B, Husband D, Joyce KA, Fildes D, Jenkinson MD, Smith T, Broome J, Kopitzki K, du Plessis DG, Prosser J, Vinjamuri S, Warnke PC (2006) Genetic and metabolic predictors of chemosensitivity in oligodendroglial neoplasms. Br J Cancer 95:1424–1431
19. Louis DN, Ohgaki H, Wiestler OD, Cavanee WK (2007) WHO classification of tumours of the central nervous system. IARC Press, Lyon
20. Le Bihan D, Breton E, Lallemand D, Grenier P, Cabanis E, Laval-Jeantet M (1986) MR imaging of intravoxel incoherent motions: application to diffusion and perfusion in neurologic disorders. Radiology 161:401–407
21. Gladson CL (1999) The extracellular matrix of gliomas: modulation of cell function. J Neuropathol Exp Neurol 58:1029–1040
22. Sadeghi N, Camby I, Goldman S, Gabius HJ, Baleriaux D, Salmon I, Decaesteckere C, Kiss R, Metens T (2003) Effect of hydrophilic components of the extracellular matrix on quantifiable diffusion-weighted imaging of human gliomas: preliminary results of correlating apparent diffusion coefficient values and hyaluronan expression level. AJR Am J Roentgenol 181:235–241
23. Beppu T, Inoue T, Shibata Y, Yamada N, Kurose A, Ogasawara K, Ogawa A, Kabasawa H (2005) Fractional anisotropy value by diffusion tensor magnetic resonance imaging as a predictor of cell density and proliferation activity of glioblastomas. Surg Neurol 63:56–61 (discussion 61)
24. Price SJ, Jena R, Burnet NG, Hutchinson PJ, Dean AF, Pena A, Pickard JD, Carpenter TA, Gillard JH (2006) Improved delineation of glioma margins and regions of infiltration with the use of diffusion tensor imaging: an image-guided biopsy study. AJNR Am J Neuroradiol 27:1969–1974
25. Stadlbauer A, Ganslandt O, Buslei R, Hammen T, Gruber S, Moser E, Buchfelder M, Salomonowitz E, Nimsky C (2006) Gliomas: histopathologic evaluation of changes in directionality and magnitude of water diffusion at diffusion-tensor MR imaging. Radiology 240:803–810